



University of
St Andrews

University of St. Andrews

Discussion papers in Environmental Economics

<http://www.st-andrews.ac.uk/gsd/research/envecon/eediscus/>

Paper 2016-05

Payment for Multiple Forest Benefits Alters the Effect of Tree Disease on Optimal Forest Rotation Length

Morag F. Macpherson, Adam Kleczkowski, John R. Healey, and Nick Hanley

Keywords: multiple-output forest, payment for ecosystem services, bioeconomic modelling, optimal rotation length, Hartman model.

JEL codes: Q23, Q54, Q57

1 Payment for multiple forest benefits alters the effect of tree disease 2 on optimal forest rotation length

3 Morag F. Macpherson^a, Adam Kleczkowski^a, John R. Healey^b and Nick Hanley^c

4 ^aComputing Science and Mathematics, School of Natural Sciences, Cottrell Building,
5 University of Stirling, Stirling, FK9 4LA UK

6 ^bSchool of Environment, Natural Resources and Geography, College of Natural Sciences,
7 Bangor University, Bangor, Gwynedd, LL57 2UW UK

8 ^cSchool of Geography & Geosciences, Irvine Building, University of St Andrews, North Street,
9 St Andrews, Fife, KY16 9AL UK

10 Abstract

11 Forests deliver multiple benefits both to their owners and to wider society. However, a wave of forest diseases
12 and pests is threatening this worldwide. In this paper we examine the optimal rotation length of a single-aged,
13 single rotation forest when a payment for non-timber benefits is included. This payment reflects the social
14 values of forest management and is offered to private forest owners to partly internalise such benefits. We show
15 that the inclusion of such a payment generally increases optimal rotation length, but this effect shows a range
16 of complex interactions with key factors linked to tree disease (its external pressure, rate of transmission and
17 impact on the value of harvested timber). Moreover, we highlight that this result is dependent on the structure
18 of the payment for non-timber benefits, and under some constraints it may be optimal to never harvest the
19 forest.

20 1 Introduction

21 Forests supply a wide range of important ecosystem services such as the regulation of hydrological and carbon
22 cycles (Cudlín et al., 2013; Carvalho-Santos et al., 2014); recreational and aesthetic values (Ribe, 1989; Nielsen
23 et al., 2007); as well as conservation of biodiversity (Johansson et al., 2013). They can also provide timber
24 revenues to private forest owners and managers. However, like many other natural resources, forests are expe-
25 riencing many challenges, one of which is the increasing pressure from novel pests and pathogens (Department
26 for Environment, Food and Rural Affairs, 2013). Changing climate (Netherer and Schopf, 2010; Pautasso et al.,
27 2010; Sturrock, 2012), globalisation of trade and the synonymous increase in the volume and diversity of plant
28 species and products being traded (Department for Environment, Food and Rural Affairs, 2013) are just a few
29 of the reasons leading to an increase in geographical ranges of pest and pathogen species. With these factors

1 unlikely to diminish in the near future, it is very important to consider the effect of disease on multiple-output
2 forests and how they are managed. More specifically, in this paper we consider the management decision of
3 clear-felling and ask: what is the effect of disease on the optimal rotation length of a multiple-benefit forest?

4 How to modify forest management to make forests less susceptible to climate change has become a popular
5 theme in the literature (Millar et al., 2007), and whilst climate and disease risks are intricately linked (Sturrock
6 et al., 2011), there appears to be far less material on the adaptation of forest management to create greater
7 protection against forest diseases. Some strategies that are reported in the literature are species diversification
8 (Perry and Maghembe, 1989; Jactel and Brockerhoff, 2007; Castagneyrol et al., 2014; Churchill et al., 2013),
9 alteration of spatial structure (Condeso and Meentemeyer, 2007) and adapting silviculture regimes such as
10 thinning (D’Amato et al., 2011; Bauce and Fuentealba, 2013). More recently, Quine et al. (2015) identified
11 33 disease management options applicable to *Dothistroma septosporum*, ranging from increasing knowledge of
12 the pathogen system to initial forest design, such as lower initial stocking density. Most of these strategies are
13 preventative and attempt to reduce the risk of initial infection. This is largely because there is little that can
14 be done to combat most pathogens once they have arrived. However, some options include: a heavier thinning
15 regime (for example against *Dothistroma septosporum* (Quine et al., 2015)); chemical sprays or biological control
16 (for example treating stumps with urea or a biological control agent *Phlebiopsis gigantea* can help prevent
17 germination and growth of aerial basidiospores causing *Heterobasidion annosum* on conifers; Johansson et al.
18 (2002)); and clear-felling the forest early (for example in the case of wide spread epidemics). All these manage-
19 ment strategies and decisions have direct implications for timber production but also for the non-timber services
20 which are attributed to forests. For example in 2013–14, 575 sites in the UK were served with a Statutory Plant
21 Health Notice requiring a total of 4.8 thousand hectares of forest to be felled in a bid to halt the progression
22 of *Phytophthora ramorum* (Forestry Commission Scotland, 2015). The removal of timber not only affects the
23 forest owner through revenue loss, but may also negatively affect the non-timber services such as habitat loss
24 which may disrupt forest wildlife (Rizzo and Garbelotto, 2003; Appiah et al., 2004). Thus when considering
25 disease, management decisions should anticipate the effect on both the timber and the non-timber benefits of a
26 forest.

27 Finding the optimal rotation length for a forest when disease is present is an economically important decision
28 for a forest manager, since the arrival of pests and pathogens can lead to losses in market values through reduction
29 in growth, for example *Dothistroma septosporum* causes significant defoliation which can greatly reduce growth
30 rate (Forestry Commission Scotland, 2013); reduction in quality, for example *Heterobasidion annosum* decays the
31 wood in the butt end of the log which may reduce the value of the timber (Pratt, 2001; Redfern et al., 2010); or
32 an increase in the susceptibility to secondary infection, for example *Hymenoscyphus fraxineus* and *Phytophthora*
33 *ramorum* cause significant damage to the bark and cambium therefore increasing the rate of infection of wood
34 decay fungi (Pautasso et al., 2013; Forestry Commission Scotland, 2015). In the case of an epidemic, large

1 areas of monoculture forest may be felled simultaneously to try to halt disease spread (as is currently taking
2 place in response to the *P. ramorum* infection of *Larix* spp. in South Wales and South West Scotland (Forestry
3 Commission Scotland, 2015)), thus a large influx of material to local sawmills may cause congestion and market
4 saturation (however we do not model this scenario explicitly as that would require a reduced price for all timber
5 independent of its infection status). In Macpherson et al. (2016) we extended a single-rotation Faustmann model
6 (which describes the net present value of a forest by including a one-off establishment cost and timber revenue;
7 Amacher et al. (2009)), and showed that the optimal rotation length of an even-aged forest is negatively affected
8 by disease. This set-up is representative of plantation forests where management decisions are driven by timber
9 production only (and non-timber values of forests are not considered). However it is commonly recognised
10 that the value of forests extend beyond timber; and Faustmann’s original model has since been extended to
11 include the benefits of non-timber goods (Hartman, 1976; Samuelson, 1976). Hartman (1976) showed that the
12 exclusion of such benefits can lead to suboptimal rotation length. Thus an important extension to Macpherson
13 et al. (2016) is to investigate the effect of disease on the optimal rotation length of a forest producing multiple
14 benefits.

15 Despite the important impact of tree pests and diseases, there is a lack of published work on the effect of
16 disease on optimal rotation length. A recent review showed that there have been 313 published books and
17 articles in over sixty journals since Faustmann’s paper on optimal rotation length analysis (Newman, 2002).
18 Some of this work includes the effect of catastrophic loss, for example from fire (Reed, 1984; Englin et al., 2000)
19 or wind blow (Price, 2011); the effect of carbon prices (Chladná, 2007; Price and Willis, 2011); the uncertainty
20 and risk of future prices (Alvarez and Koskela, 2006; Loisel, 2011; Sims and Finnoff, 2013); and multiple forests
21 and their interdependent provision of amenity services (Koskela and Ollikainen, 2001). The arrival of disease
22 could be considered a catastrophic event in the case of widespread epidemics where large areas of forest are
23 felled and timber and non-timber benefits (such as ecosystem services) are affected. However, there are many
24 dissimilarities when comparing the effect of disease to the classic catastrophic events such as fire and wind (see
25 Macpherson et al. (2016) for these comparisons), and a separate analysis is beneficial.

26 In this paper we extend the model in Macpherson et al. (2016) by assuming that the forest owner has an
27 interest in non-timber benefits such as biodiversity, carbon sequestration or recreation. A “green” payment (a
28 form of payment for ecosystem services) is used to provide an economic incentive for the private forest owner
29 to take into account the non-timber benefits of retaining tree cover when making decisions. Therefore the net
30 present value (NPV) of the forest is similar to a (single-rotation) Hartman model since it includes a one-off
31 establishment cost, timber revenue and a non-timber, green payment. However, we now assume that the disease
32 will reduce the value of timber from infected trees, thus the timber revenue and NPV of the forest is dependent
33 on the infection state of the forest at the time of harvesting (in addition to the volume of timber). In order to
34 include the epidemiology we define a system of first order differential equations describing the rate of change of

1 area of infection over time and proceed by finding the first order condition of the NPV. Despite being unable to
2 analytically derive the optimal rotation length, the first order condition and numerical optimisation can provide
3 significant insight into the system's dynamics and sensitivity to key parameters.

4 Our key question is to analyse the effect of disease on the optimal rotation length of a forest managed for
5 multiple benefits. Initially we assume that the green payment is only dependent on the total area of forest covered
6 by unharvested trees and not on the infection status. This is reasonable since not all diseases severely disturb
7 the forest ecosystem or the provision of services. For example, diseases which reduce the growth rate of trees,
8 such as *Dothistroma septosporum* on *Pinus* spp., may decrease the timber revenue but have a limited impact on
9 the non-timber benefits (except for the rate of carbon sequestration associated with tree growth). Alternatively,
10 it is clear that some diseases do cause a decline in non-timber benefits such as the loss of biodiversity, and
11 recreation and aesthetic values, and a much greater impact on carbon storage (Boyd et al., 2013; Department
12 for Environment, Food and Rural Affairs, 2013), therefore we investigate how the green payment can be adapted
13 to depend on the specific impacts of a disease. This meets a second key aim, to analyse the effect of disease on
14 the optimal rotation length when we consider different structures of green payments.

15 The structure of this paper is as follows. In section 2 we define the first-order condition for a single rotation
16 Hartman model and then extend the framework to include a general disease system. In section 3 we introduce
17 a specific forest volume function and susceptible-infected (SI) disease system, which we use to highlight some
18 key results produced by numerical optimisation in section 4. In section 5 we briefly discuss the effect of a green
19 payment which depends on the extent of disease spread in the forest.

20 **2 Formulation of the general model**

21 **2.1 The model without disease**

22 We develop a single rotation Hartman model of the NPV of an even-aged, monoculture forest which includes
23 the establishment cost (planting from bare land), the benefit from harvesting the timber, and a non-timber
24 green payment (Hartman, 1976). We assume that for a forest of area L (in hectares), the establishment costs
25 are linearly dependent on the area, $W(L) = cL$ where c is the planting cost per hectare. The net benefit of
26 harvesting, $M(L, T)$, is a product of the per-cubic-metre price of timber, p , and the volume of timber produced,
27 $f(T)L$. The annual green payment is linearly dependent on the area of the forest, $S(L) = sL$ where s is the
28 payment per hectare per year and is obtained for as long as the trees remain unharvested. Further underlying
29 assumptions include: all costs and prices are constant and known; future interest rates are constant and known;
30 and the timber volume function of the species are known (Amacher et al., 2009). Thus the NPV of a forest

1 with a rotation length of T years is

$$\hat{J}(T) = -W(L) + M(L, T)e^{-rT} + \int_0^T S(L)e^{-rt} dt. \quad (1)$$

2 An exponential discount factor, with rate r , is used to discount future revenue, from the timber harvest and the
 3 green payment, back to the time of planting. Parameter definitions and baseline values are given in Table 1. To
 4 find the optimal rotation length which maximises the NPV, we find the first-order condition by differentiating
 5 Equation (1) with respect to T which gives

$$\frac{d\hat{J}(T)}{dT} = \frac{dM}{dT}e^{-rT} - rM(L, T)e^{-rT} + S(L)e^{-rT}. \quad (2)$$

6 Setting Equation (2) equal to zero and substituting the function for the revenue from harvesting we obtain

$$\frac{1}{f(T_{DF})} \frac{df}{dT} \Big|_{T=T_{DF}} - r = -\frac{S(L)}{pLf(T_{DF})}. \quad (3)$$

7 This implies that the optimal rotation length for the disease free system ($T = T_{DF}$), which maximises the
 8 NPV, is given when the marginal gain from the relative growth in timber volume and the opportunity cost of
 9 investment (left-hand side) is equal to the non-timber benefits relative to the timber revenue (right-hand side).
 10 The green payment is designed to increase the benefit of retaining the cover of the current tree crop unharvested
 11 for longer, and Equation (3) shows this since an increase in the green payment will increase the benefit obtained
 12 from delaying the harvest, and therefore increase the optimal rotation length.

13 Evaluating the second derivative at the optimal rotation length gives

$$\frac{d^2\hat{J}}{dT^2} \Big|_{T=T_{DF}} = pLe^{-rT_{DF}} \left(\frac{d^2f}{dT^2} \Big|_{T=T_{DF}} - r \frac{df}{dT} \Big|_{T=T_{DF}} \right) < 0 \quad (4)$$

14 which holds if timber volume has an increasing, concave function.

15 2.2 General model with disease

16 We now examine the effect of disease on the optimal rotation length. By scaling the revenue obtained from
 17 timber of infected trees appropriately, we can represent the reduction in timber value caused by disease. We
 18 first introduce the NPV and the general disease system, and finally derive the first-order condition which allows
 19 us to show the effect of disease on the optimal rotation length.

20 Equation (1) represents the NPV for a forest of area L which remains disease free. We build on this model,
 21 by assuming that the revenue obtained from the timber is dependent on the state of infection at that point in

1 time. Therefore the NPV can be given by

$$\hat{J}(T) = -W(L) + M(\tilde{L}(T), T)e^{-rT} + \int_0^T S(L)e^{-rt} dt \quad (5)$$

2 where $\tilde{L}(T)$ denotes the effect of the disease on the total area of the forest (explained further below). The
 3 establishment cost and green payment remain unchanged by disease. Furthermore, no action is taken to prevent
 4 or treat disease spread and therefore there are no additional costs (for example through control or treatment).

Next we assume that a general disease system with N stages of progress is introduced to the forest. We denote the area of the forest covered by the tree crop in the i th stage by $x_i(T)$ where $1 \leq i \leq N$, and since no partial felling is undertaken the area of tree cover is conserved giving $L = \sum_{i=1}^N x_i(T)$. If the disease has no effect on the timber, the revenue from timber in the i th stage of infection is $pf(T)x_i(T)$. However, we assume that the disease reduces the value of timber (either through reduced quality or growth), so the revenue from timber at each stage is scaled by parameter ρ_i where $0 \leq \rho_i \leq 1$. This means that timber may be affected differently by disease at each stage. We can therefore represent the harvest revenue function for the forest as

$$M(\tilde{L}(T), T) = pf(T) \left(\sum_{i=1}^N \rho_i x_i(T) \right) \quad (6a)$$

$$= pf(T) \tilde{L}(T) \quad (6b)$$

5 where the effect of disease on the whole forest at time T is given by

$$\tilde{L}(T) = \sum_{i=1}^N \rho_i x_i(T). \quad (7)$$

Since the disease spreads throughout the forest as time increases, we specify a system of differential equations (dx_i/dt) which can be solved for $x_i(t)$, and substituted into the harvest revenue function (Equation (6b)). We are then able to proceed as before and find the optimal rotation length using the first-order condition. We can find a general solution by differentiating Equation (5) which gives

$$\frac{d\hat{J}(T)}{dT} = e^{-rT} \frac{d}{dT} \left(M(\tilde{L}(T), T) \right) - re^{-rT} M(\tilde{L}(T), T) + (S(L)) e^{-rT} \quad (8a)$$

$$= pe^{-rT} \left(\frac{S(L)}{p} + p \frac{df}{dT} \tilde{L}(T) + pf(T) \frac{d\tilde{L}(T)}{dT} - rf(T) \tilde{L}(T) \right). \quad (8b)$$

6 Setting Equation (8b) equal to zero and re-arranging we have

$$\frac{1}{f(T_D)} \frac{df(T)}{dT} \Big|_{T=T_D} - r = \frac{1}{\tilde{L}(T_D)} \left(\left. \frac{d\tilde{L}}{dT} \right|_{T=T_D} - \frac{S(L)}{pf(T_D)} \right). \quad (9)$$

Equation (9) shows that the optimal rotation length ($T = T_D$) is obtained when the relative marginal benefit of waiting for one more instant of timber growth minus the discount rate (left-hand side) is equal to the relative marginal cost of the disease spreading further and the benefit of accruing the green payment (right-hand side). We note that the left-hand side of this equation is the same as the system without disease (Equation (3)), and see that in the absence of a green payment the inclusion of the disease will reduce the optimal rotation length since $\tilde{L}(T)$ is a decreasing function (Macpherson et al., 2016). When the green payment is positive, that is the owner benefits from the non-timber values of the forest, the optimal rotation length will increase, but without knowing the magnitude of the terms (on the right-hand side) it is impossible to say what the net outcome will be (compared with the disease-free case).

Evaluating the second derivative at the optimal rotation length gives

$$\left. \frac{d^2 \hat{J}(T)}{dT^2} \right|_{T=T_D} = \left[pe^{-rT} \left(\tilde{L}(T) \left(\frac{d^2 f}{dT^2} - r \frac{df}{dT} \right) + 2 \frac{d\tilde{L}}{dT} \frac{df}{dT} + f(T) \left(\frac{d^2 \tilde{L}}{dT^2} - r \frac{d\tilde{L}}{dT} \right) \right) \right]_{T=T_D}. \quad (10)$$

The sign of Equation (10) is unclear and dependent on the relative magnitude of the terms. Once the disease system is specified, we can show that the optimal rotation length is always a maximum.

3 A numerical model

In order to examine the sensitivity of the optimal rotation length to changes in the disease parameters, we specify the timber volume growth, $f(T)$, in section 3.1 and the disease system, $\tilde{L}(T)$, in section 3.2

3.1 Timber volume function

In our framework the net benefit at the end of the rotation is dependent on the function describing the volume of timber, $f(T)$. In this paper we use a typical yield class 14 to define the growth rate of *Picea sitchensis* (sitka spruce) since it is the dominant conifer species grown in Scotland and elsewhere in the British uplands (Forestry Commission, 2011). The Forest Yield model developed by the government agency Forest Research was used to estimate the average timber volume per tree and density of trees (number per hectare) over time (Forest Research, *Private communication*, 2015), which allowed us to estimate the average timber volume per hectare. These data points are shown in Figure 1 (a) where the timber volume for a hectare of forest (V_i) is given for each time step (T_i). (T_1, V_1) is the point recorded when the average tree has grown into the 7 – 10 cm range of diameter at breast height (DBH); trees are generally not commercially harvested at smaller sizes. This model includes the natural mortality rate that is expected of an un-thinned stand with 2 m initial tree spacing.

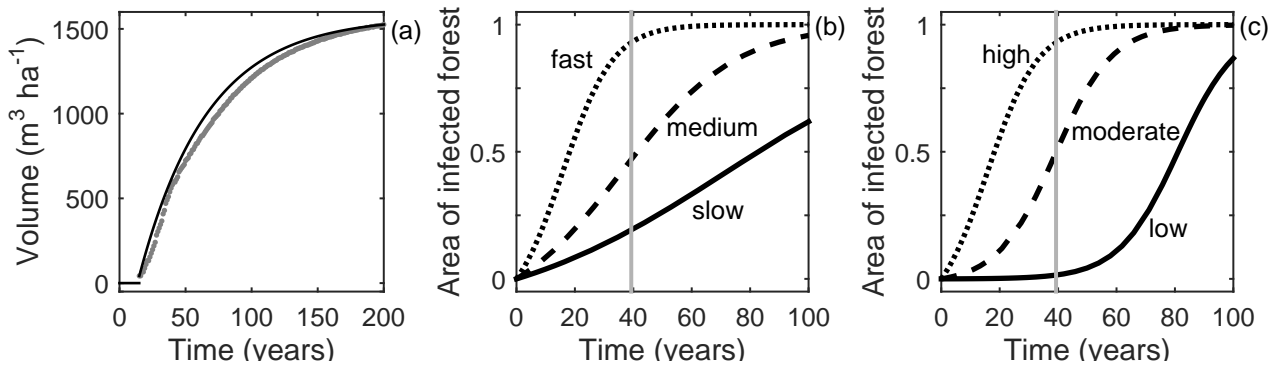


Figure 1: Timber volume growth function and disease progress curves. In (a) the data points of timber volume growth (grey dots) from the Forest Yield model are given for unthinned, yield class 14 *Picea sitchensis*. The fitted curve (black) is produced using Equation (11) and the parameters are given in Table 1. Separately, the modelled area of forest with infected trees ($L - x(t)$) against time is plotted with (b) fixed external pressure and three values of disease transmission and (c) fixed disease transmission and three values of external pressure (the parameter sets are given in Table 2). The optimal rotation length of the disease-free system, T_{DF} , is shown as a vertical grey line.

1 Using the model output we can fit a curve which has the form

$$f(T) = \begin{cases} 0 & \text{if } T < T_1 \\ V_M \left(1 - e^{\bar{b}(T-T_1)}\right) + V_1 & \text{if } T \geq T_1. \end{cases} \quad (11)$$

2 where (T_M, V_M) is the last data point. Forest Yield gave 185 years of output and in order to capture the shape
3 of the curve over time we fit parameter \bar{b} by setting $f(200) = V_M$. Moreover, since we are examining the effect
4 of disease on the optimal rotation length, we include the full time horizon output. All parameter values are
5 given in Table 1, and Figure 1 (a) shows the data points and fitted curve given by Equation (11). Since trees are
6 generally only harvested after they have reached 7 – 10 cm DBH, our model uses T_1 as a minimum harvesting
7 boundary (which we refer to throughout this paper), where the trees cannot be harvested before this time point.

8 3.2 Susceptible-Infected disease system

We now reduce the N -state epidemiological equations to a two-state, Susceptible-Infected (SI) system with $x(t)$ representing the area of the susceptible (not infected) part of the forest and $y(t)$ the area of the infected part of the forest. The total area of forest remains constant over time ($L = x(t) + y(t)$), therefore the SI system can be written as

$$\frac{dx}{dt} = -\beta x(t)(y(t) + P) \quad (12a)$$

$$\frac{dy}{dt} = \beta x(t)(y(t) + P) \quad (12b)$$

L	Area of forest	$L = 1$ ha
c	Forest establishment cost	$c = \text{£}1920 \text{ ha}^{-1}$ **
p	Price of timber	$p = \text{£}17.90 \text{ m}^{-3}$ ***
s	Annual green payment	$\text{£}100 \text{ ha}^{-1}$
r	Discount rate	$r = 0.03$
$f(T)$	Timber volume growth ($\text{m}^3 \text{ ha}^{-1}$)	Equation (11)
(T_i, V_i)	Time, T_i (years), and volume, V_i , ($\text{m}^3 \text{ ha}^{-1}$) from Forest Yield *	$(T_1, V_1) = (15, 43)$
\bar{b}	Fitted parameter in timber volume growth function $f(T)$	$\bar{b} = -0.01933$ *
$\tilde{L}(T)$	Impact of disease on the whole forest at time T	Equation (6)
β	Disease transmission coefficient	Table 2
P	External inoculum pressure from disease	Table 2
$t_{0.5}$	Time taken for the susceptible area to halve	Table 2
ρ	Revenue of timber from infected trees relative to that from uninfected trees	$0 \leq \rho \leq 1$

Table 1: Parameter definition and baseline values used in this paper. Parameters marked * denote values taken from the Forest Yield model of the Forest Research agency in Great Britain for yield class 14 *Picea sitchensis* without thinning and with a 2-m initial spacing ($2500 \text{ trees ha}^{-1}$). The net cost of planting (marked **) is taken to be zero on the basis that the gross cost is the same as the government subsidy payments available through a ‘Woodland creation’ scheme (in the form of an initial planting payment; <https://www.ruralpayments.org/publicsite/futures/topics/all-schemes/forestry-grant-scheme/woodland-creation/>). The price of timber (marked ***) is the average standing price (per cubic metre overbark) taken from Coniferous Standing Sales Price Index on 30th September 2014 for Great Britain (<http://www.forestry.gov.uk/forestry/INFD-7M2DJR>).

1 where disease is introduced to an initially susceptible population ($x(0) = L$) by an external inoculum pressure
2 P (for example, by spores of the pathogen being dispersed to the forest), and disease transmission from infected
3 to susceptible trees is controlled by the transmission coefficient β . Since the area of forest is conserved ($dL/dt =$
4 $dx/dt + dy/dt = 0$) we can eliminate Equation (12b) by setting $y(t) = L - x(t)$. Thus the system reduces to a
5 one-state equation

$$\frac{dx}{dt} = -\beta x(t)(L - x(t) + P), \quad (13)$$

6 which can be solved using the separation of variables method to give

$$x(t) = \frac{L + P}{\frac{P}{L}e^{(L+P)\beta t} + 1}. \quad (14)$$

7 In the general framework, $\tilde{L}(t)$ is used to represent the effect of disease on the whole forest (Equation (6)). For
8 the SI system we have

$$\tilde{L}(t) = x(t) + \rho(L - x(t)) \quad (15)$$

9 where ρ scales the revenue from timber that is infected ($0 \leq \rho \leq 1$). Setting $\rho = 1$ means that the disease has
10 no effect on the timber revenue from infected trees; conversely $\rho = 0$ means that the timber from infected trees
11 is worth nothing since $\tilde{L}(t) = x(t)$.

12 The disease dynamics in Equation (14) are governed by the transmission coefficient and an external inoculum
13 pressure (henceforth ‘external pressure’). We select six parameter sets (detailed in Table 2), which aim to capture

Disease dynamics (transmission – external pressure)	β	P	$t_{0.5}$
Fast – high	0.1	0.16*	$t_{0.5} = T_{DF}/2$
Medium – high	0.044	0.16	$t_{0.5} = T_{DF}$
Slow – high	0.022	0.16	$t_{0.5} = 2T_{DF}$
Fast – high	0.1*	0.16	$t_{0.5} = T_{DF}/2$
Fast – moderate	0.1	0.019	$t_{0.5} = T_{DF}$
Fast – low	0.1	0.0003	$t_{0.5} = 2T_{DF}$

Table 2: The disease parameter sets for each level of transmission coefficient, β (‘fast’, ‘medium’ and ‘slow’) and external pressure of disease, P (‘high’, ‘moderate’ and ‘low’). $t_{0.5}$ is the time taken (in years) for the infection to spread to half of the forest as described in Equation (16). Disease progress curves for each parameter set are shown in Figure 1 (b) and (c). T_{DF} is the optimal rotation length in the absence of disease and subsidies. * denotes the baseline value for the external pressure and disease transmission.

1 the characteristics of different diseases caused by different pathogen species. It may be possible to estimate
2 transmission coefficients from epidemiological field data, however interpreting and quantifying an appropriate
3 value of external pressure is more difficult. We therefore introduce another parameter $t_{0.5}$, which is the time
4 taken for half of the forest to become infected, to describe the external pressure (by fixing the disease transmission
5 coefficient). Using Equation (14) we can find this value by setting $x(t_{0.5}) = 0.5L$ giving

$$t_{0.5} = \frac{\ln(L/P + 2)}{(L + P)\beta}. \quad (16)$$

6 We can equate $t_{0.5}$ to the disease-free rotation length, or proportions of it, to allow for an easy interpretation
7 of the effect of variation in external pressure (when the disease transmission is fixed). For example, $t_{0.5} = T_{DF}$
8 would translate to, half the trees in the forest being infected by the end of a disease-free rotation. Figures 1 (b)
9 and (c) show disease progress curves generated for the parameter sets in Table 2. (Note that we also give $t_{0.5}$
10 for the first set of parameters when P is constant and β is fixed – this was done in order to find appropriate
11 levels of β .)

12 4 General results

13 In this section we use the timber volume function and disease system defined in section 3 to give further insight
14 into the results found in section 2. Many of the results cannot be obtained analytically, however we highlight
15 key trends which demonstrate the intricate relationship between the green payment and disease dynamics.

16 4.1 No disease

17 First we analyse the system without disease to provide baseline results which can be used to measure the effect
18 of disease on the system. Recalling that the optimal rotation length is given by the first-order condition in

1 Equation (3), we now substitute the timber volume function (Equation (13)) to obtain

$$-\frac{\bar{b}V_M e^{\bar{b}(T-T_1)}}{V_M(1 - e^{\bar{b}(T-T_1)}) + V_1} - r = -\frac{s}{p(V_M(1 - e^{\bar{b}(T-T_1)}) + V_1)}. \quad (17)$$

2 Solving for the optimal rotation length ($T = T_{DF}$) we have

$$T_{DF} = \frac{1}{\bar{b}} \ln \left(\frac{s - pr(V_M + V_1)}{pV_M(\bar{b} - r)} \right) + T_1 \quad (18)$$

3 which exists when $pr(V_M + V_1) > s$, since $\bar{b} < 0$. When the value of the green payment when is greater than
4 this (let (let $s^{(\infty)}$ be the value where $s = pr(V_M + V_1)$) then the optimal rotation length will be infinite. When
5 $s < s^{(\infty)}$, the optimal rotation length is where the maximum NPV is achieved; that is where waiting for one more
6 instant of timber growth and non-timber benefits (through the green payment) is equal to the opportunities
7 forgone (the profit which could be obtained from investing elsewhere, such as a bank). From Equation (18)
8 we see that an increase in green payment, s , will increase the optimal rotation length and maximum NPV.
9 This is also shown in Figure 2 (a) where the NPV is plotted against the rotation length, T . The relationship
10 between optimal rotation length and the green payment is shown further in Figure 2 (b) where it is clear
11 that, as $s \rightarrow s^{(\infty)}$, then $T_{DF} \rightarrow \infty$, with the optimal rotation length becoming infinite. This results in the
12 optimal strategy changing from clear-felling to not harvesting, thus altering the forest to a complete amenity
13 or protection forest (producing only non-timber benefits).

14 4.2 Disease

15 We now find the optimal rotation length for the system with disease, $T = T_D$, which maximises the NPV
16 in Equation (5) when the forest volume function is of the form of Equation (13), and the disease follows the
17 susceptible-infected framework shown in Equation (14). We know that disease reduces the optimal rotation
18 length in the absence of a green payment (Macpherson et al., 2016), however without disease, the inclusion of
19 a green payment increases the optimal rotation length (Figure 2), thus creating a trade-off in the effects of the
20 green payment and the cost of the disease. An analytical solution for the optimal rotation length is intractable,
21 therefore we divide the system into two scenarios to carry out sensitivity analyses to the parameters controlling
22 the disease spread (β and P , by setting $\rho = 0$) in section 4.2.1, and the revenue from timber that is infected (ρ ,
23 by setting $0 \leq \rho \leq 1$) in section 4.2.2. We only consider the parameter space greater than the minimum tree
24 size harvesting boundary ($T \geq T_1$).

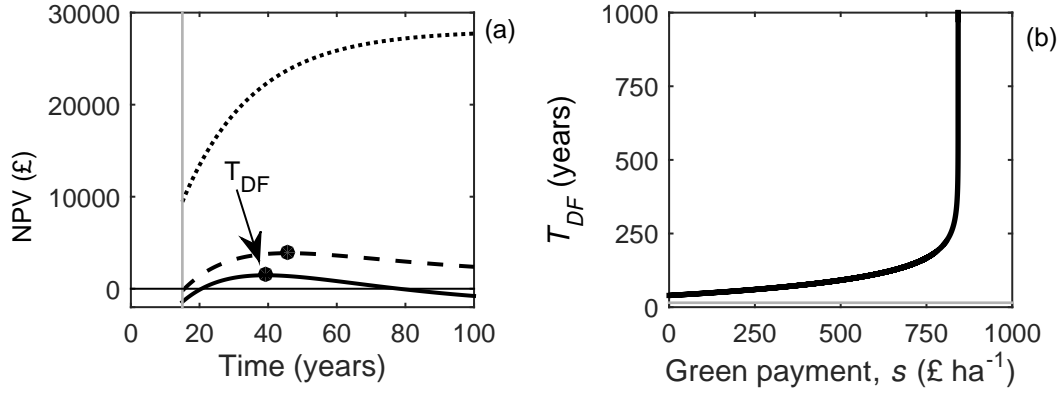


Figure 2: The effect of a green payment for non-timber benefits on the optimal forest rotation length. In (a) the NPV in Equation (1) against time for three levels of green payment per hectare per year, $s = 0$ (solid black), $s = 100$ (dashed black) and $s = 900$ (dotted black). A black circle marks the optimal rotation length which maximises the NPV for the first two cases (this was never reached in the time period shown in the third case), and T_{DF} identifies the optimal rotation length when $s = 0$. In (b) the variation in the optimal rotation length (T_{DF}) with the rate of green payment, s (in £ ha⁻¹ year⁻¹). Note that when green payments are greater than $s^{(\infty)} = 843.55$ the optimal rotation length becomes infinite. In all plotted relationships the growth function is parameterised for yield class 14 *Picea sitchensis* where the minimum harvesting boundary, T_1 (the time where the average tree grows into the 7-10 cm DBH size class), is given by the vertical grey line in (a) and horizontal grey line in (b). Other parameters can be found in Table 1.

4.2.1 Sensitivity analysis to the disease characteristics

Setting $\rho = 0$ simplifies the model, as the net benefit of the timber at the end of the rotation is dependent on the area of healthy forest only, that is $\tilde{L}(T) = x(t)$ from Equation (7). Substituting this and the timber volume function (Equation (13)) into the first order condition in Equation (9), we find

$$\frac{1}{f(T)} \frac{df}{dT} - r = \frac{1}{x(T)} \left| \frac{dx}{dT} \right| - \frac{S(L)}{pf(T)x(T)} \quad (19a)$$

$$\frac{-V_M \bar{b} e^{\bar{b}(T-T_1)}}{V_M(1 - e^{\bar{b}(T-T_1)}) + V_1} - r = \frac{P\beta(L+P)}{P + L e^{-(L+P)\beta T}} - \frac{s(Pe^{(L+P)\beta T} + L)}{p(L+P)(V_M(1 - e^{\bar{b}(T-T_1)}) + V_1)}. \quad (19b)$$

Whilst we are unable to solve Equation (19b) analytically, we can use numerical optimisation to plot the optimal rotation length ($T = T_D$) against the green payment in Figure 3 (a). It is clear that the green payment has a positive effect on the optimal rotation length for the four disease parameter sets shown (no disease, slow, medium and fast disease transmission), and the disease has a negative effect on the optimal rotation length (for each green payment value the optimal rotation length, when it exists, decreases as the disease transmission is increased). A key point illustrated in Figure 3 (a) is that, like in the disease-free case, once a critical value of green payment is realised (say $s_D^{(\infty)}$, identified by the circles), it becomes optimal to never harvest the forest. This occurs for the following reason. Without a green payment the (negative) NPV is initially equal to the establishment costs. As time passes the trees grow and the revenue from selling the timber increases, however

1 the timber volume growth eventually saturates (Figure 1 (a)), and thus the NPV reaches a maximum. If the
2 trees are not harvested, the timber revenue will then decrease as $T \rightarrow \infty$ (due to a decline in timber growth,
3 discounting and disease), and the NPV tends to the establishment costs, $W(L)$. Thus there is always one global
4 stationary point in time which maximises the NPV (the “optimal rotation length”). The inclusion of a green
5 payment, however, adds additional revenue (independent of tree growth and infection status) for as long as the
6 trees remain unharvested, and we find that as $T \rightarrow \infty$ then $\hat{J} \rightarrow S(L)/r - W(L)$. Therefore when the green
7 payment is large enough, $S(L)/r - W(L)$ will be greater than the value obtained at any other point in the
8 rotation and thus it is optimal not to harvest.

9 We noted that in the disease-free case (Equation (18)) an infinite optimal rotation length was produced as
10 $s \rightarrow s^{(\infty)}$. However, when disease is included the switch to an infinite rotation length occurs for much smaller
11 green payments, $s_D^{(\infty)} < s^{(\infty)}$, since disease reduces the revenue from the harvested timber and decreases the
12 benefit from delaying harvest. (Equation (19a) also shows this since the green payment term is scaled by the
13 area of uninfected trees, $1/x(T)$.) For the disease-free case we analytically found the green payment value, $s^{(\infty)}$,
14 however due to the complexity of the system we cannot find the green payment value which triggers the switch.

15 Figure 3 (b) also highlights the interaction between the effects of disease and the green payment by plotting
16 the maximum NPV against the green payment value for the disease parameter sets. The decrease in the
17 maximum NPV due to disease is clear (by fixing the green payment and comparing the maximum NPV for each
18 curve), and in some cases, despite harvesting at the optimal time, the maximum NPV is negative (this is true
19 for the fast transmission case in Figure 3 (b)). Increasing the green payment can offset some of the losses made
20 from disease, however the maximum NPV for the system without disease is never achieved (for the same green
21 payment).

22 Further analysis in Figure 3 (c) shows the optimal rotation length for the system with disease, T_D , against
23 green payment values and disease transmission (with fixed external pressure). Taking a horizontal transect (i.e.
24 fixing the disease transmission) we can see that, as before, increases in the green payment lead to increases in
25 the optimal rotation length which, once a critical green payment is reached, switches to infinity (represented
26 by the black parameter space). Taking a vertical transect (i.e. fixing the green payment) we see that, as the
27 disease transmission is increased, the optimal rotation length decreases as it approaches the parameter space
28 where $T_D = \infty$. We note that on the x-axis, the system simplifies to the disease-free case (since $\beta = 0$), and the
29 optimal rotation length (for the system with disease) will not be greater than the system without disease when
30 it exists. Moreover, the parameter space where $T_D = \infty$ (coloured black in Figure 3 (c)) will meet the x-axis at
31 $s = s^{(\infty)}$ (as would be seen if the x-axis range was extended).

32 We have carried out a similar sensitivity analysis to the external pressure of Equation (5), with $\rho = 0$, and
33 it showed that increasing the external pressure had a similar effect on the optimal rotation length as increasing
34 the disease transmission. More specifically, a disease which arrives early and transmits slowly has a similar

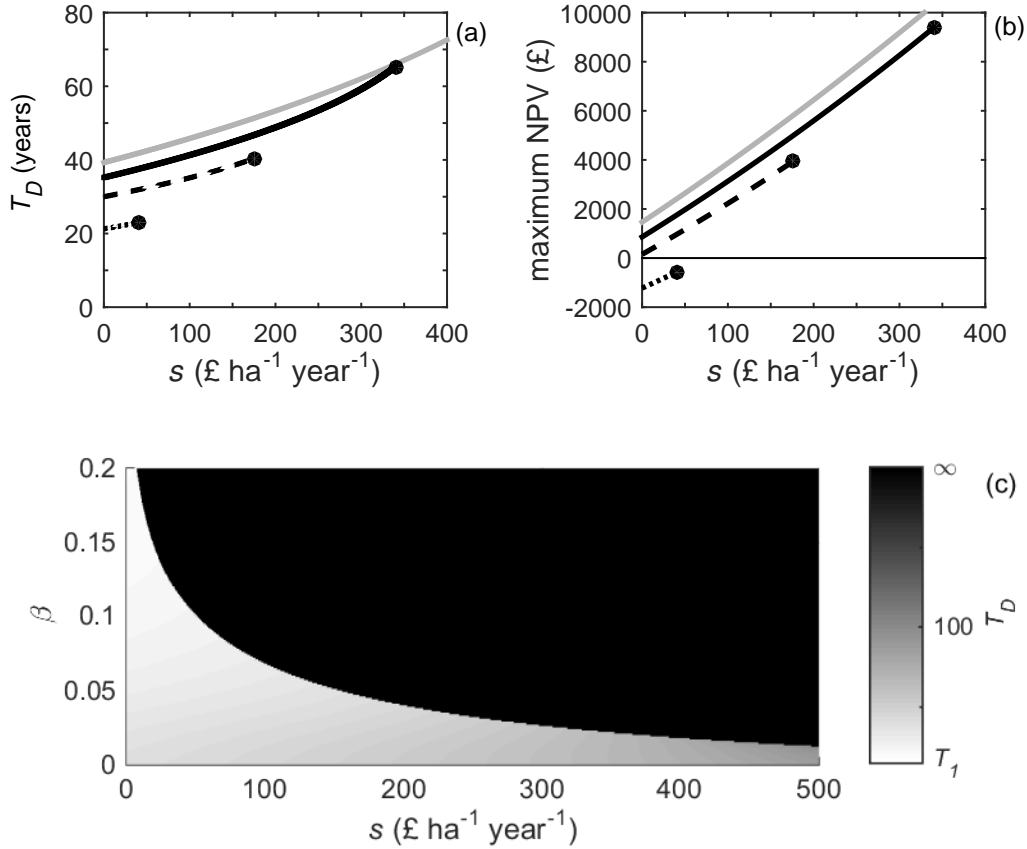


Figure 3: The effect of disease transmission on the optimal rotation length. Variation in (a) the optimal rotation length, T_D , and (b) the maximum NPV in Equation (5) with the level of green payment s (£ ha⁻¹ year⁻¹). The external pressure of the disease is set at the baseline value. Three levels of transmission coefficient, slow (solid black), medium (dashed black) and fast (dotted black), with parameter values as defined in Table 2, are shown, together with the system without disease (grey line; Equation (1)). The black circles indicate the green payment value where the optimal rotation length becomes infinite. This analysis is extended in (c) where the optimal rotation length is shown as the gradation in black-white shading across the $s - \beta$ (green payment–disease transmission) parameter space. The grey-scale on the right-hand side indicates the optimal rotation length (T_D) with the lower boundary equal to the minimum harvesting boundary, T_1 (white) and the upper boundary equalling an infinite rotation length (black). Other parameters can be found in Table 1 and $\rho = 0$.

1 effect on the optimal rotation length to a disease which arrives late and transmits fast.

2 4.2.2 Sensitivity analysis to the revenue from timber that is infected

In the previous scenario we assumed that the market value of timber from infected trees is zero ($\rho = 0$). However, it is possible that timber from infected trees can still create some revenue, and in this section we aim to understand how this can influence the optimal rotation length for a forest delivering multiple benefits. Using the same method as before we substitute the function describing the infected forest, $\tilde{L}(t) = x(t)(1 - \rho) + \rho L$,

and timber volume function (Equation (13)) into the first order condition (Equation (9)) and get

$$\frac{1}{f(T)} \frac{df}{dT} - r = \frac{1}{\tilde{L}(T)} \left(\left| \frac{d\tilde{L}(T)}{dT} \right| - \frac{S(L)}{pf(T)} \right) \quad (20a)$$

$$\frac{-V_M \bar{b} e^{\bar{b}(T-T_1)}}{V_M(1 - e^{\bar{b}(T-T_1)}) + V_1} - r = \frac{P e^{(L+P)\beta T} + L}{L + P(1 + \rho(e^{(L+P)\beta T} - 1))} \left(\frac{\beta P(L + P)^2 e^{(L+P)\beta T} (1 - \rho)}{(P e^{(L+P)\beta T} + L)^2} - \frac{s}{p(V_M(1 - e^{\bar{b}(T-T_1)}) + V_1)} \right). \quad (20b)$$

Equation (20b) is analytically intractable, however we use numerical optimisation (as before) for analysis of the sensitivity of the optimal rotation length to ρ . An increase in the green payment will increase the optimal rotation length independently of the disease characteristics and the value of timber from infected trees (Figure 4). However, it is interesting that for a level of green payment, decreasing the value of timber from infected trees can result in either an increase or a decrease in the optimal rotation length. For example, when the disease spread is slow, as ρ is decreased from 1 to 0 the optimal rotation length decreases when $s \leq 200$, but increases when $s = 400$ (Figure 4 (a)). When the disease transmission is fast the behaviour is the same, although a smaller green payment is required for the optimal rotation length to increase (a payment of $s = 100$ is sufficient; Figure 4 (b)). This trend can be seen further in Figures 4 (c) and (d) where the optimal rotation length is shown in a $s - \rho$ parameter space for a slow- and fast-transmitting disease respectively. As the value of timber from infected trees is decreased, the optimal rotation length will change depending on whether the green payment, s , is less than or greater than $s_D^{(\infty)}$ (the green payment required for the optimal rotation length becomes infinite when $\rho = 0$). When the green payment is less than $s_D^{(\infty)}$ the optimal rotation length will decrease as ρ is decreased. Alternatively, when the green payment is greater than $s_D^{(\infty)}$, the optimal rotation length will increase as ρ is decreased and eventually become infinite (black area in parameter space in Figures 4 (c) and (d)).

Figure 4 highlights the complex interaction between the disease spread, the effect of disease on timber value, and the green payment. The decline in the optimal rotation length as the timber value of infected trees decreases is easily understood, because the NPV is reduced thus motivating an earlier harvest to increase the proportion of timber from uninfected trees. The increase in the optimal rotation length when $s > s_D^{(\infty)}$ can be understood as the non-timber benefits, which is dependent on the retention of unharvested trees, outweighing the timber benefits. When the disease spreads quickly (Figures 4 (b) and (d)), most of the forest is infected by the time the trees have grown above the minimum tree size harvesting boundary, and thus a majority of the timber is subject to the reduced timber value. Therefore, there is a benefit in letting the trees grow further before harvest and thus accrue the green payment for non-timber benefits. When the disease spreads slowly (Figures 4 (a) and (c)) the effect of the disease on the timber benefits is less, thus a greater annual green payment value is required to motivate delaying harvest.

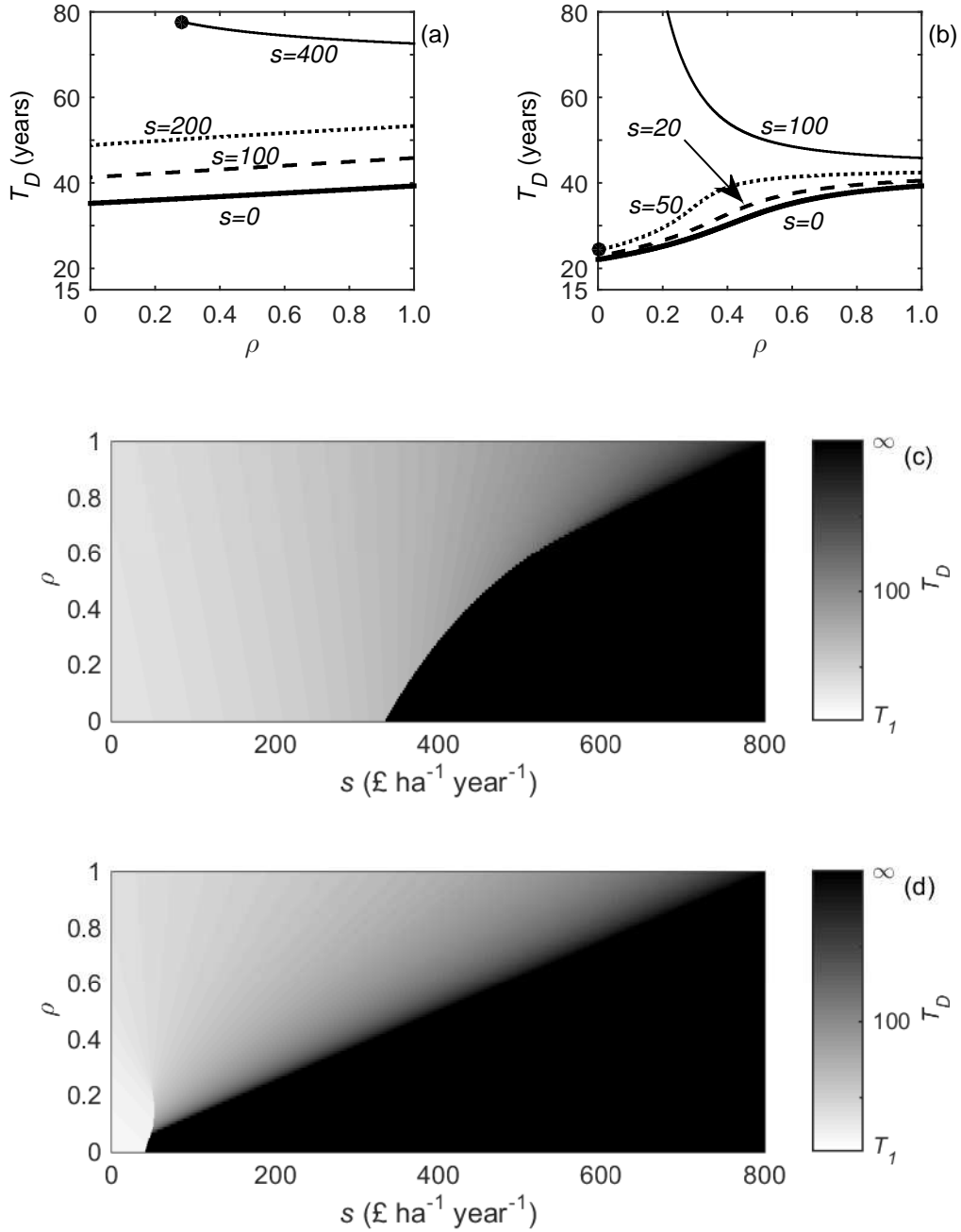


Figure 4: Variation in the optimal rotation length, T_D , with the value of timber from infected trees relative to the value from uninfected trees, ρ , for (a) a slow-transmitting disease and (b) a fast-transmitting disease. The value of the green payment, s (£ ha⁻¹ year⁻¹), is given next to each curve. The optimal rotation length, T_D , is shown as the gradation in black-white shading across the $s - \rho$ parameter space (corresponding to variation in the relative value of harvested timber from infected trees and green payments for non-timber benefits) for (c) a slow transmitting disease and (d) a fast transmitting disease. The grey-scale on the right-hand side indicates the optimal rotation length (T_D) with the lower boundary equal to the minimum harvesting boundary, T_1 (white) and the upper boundary equalling an infinite rotation length (black). The external pressure is at the baseline. In all figures, the external pressure is at the baseline value (see Table 2), and all other parameters are given in Table 1.

1 5 The effect of disease on the green payment

2 So far we have assumed that the non-timber benefits remain unaffected by disease. We now investigate what
 3 happens when the green payment is dependent on the infection state of the forest, that is $S(L) = s\tilde{L}(T)$ in
 4 Equation (5). This means that as the disease spreads throughout the forest, both the timber benefit and the
 5 green payment will decrease (as would be the case, for instance, if the payment was based on the rate of carbon
 6 sequestration through tree growth); meaning that waiting for one more instalment of green payment is less
 7 desirable (compared with the case where disease does not affect the green payment).

8 Substituting $S(L) = s\tilde{L}(T)$ in to Equation (5) we can carry out a sensitivity analysis to the disease transmis-
 9 sion by setting $\rho = 0$ (so $S(L) = sx(T)$) in Figure 5. As usual, increasing the value of the disease transmis-
 10 sion parameter decreases the optimal rotation length since there is an advantage to harvesting earlier due to the
 11 decreasing value of timber *and* in this case non-timber benefits. When the green payment is independent of
 12 disease (section 4.2.2), we found that the optimal rotation length became infinite, with a faster disease trans-
 13 mission requiring a smaller green payment (Figure 3 (c)). In contrast, the opposite is now true: compared to
 14 the system without disease (e.g. along the x-axis), a much larger green payment is required ($s > s^{(\infty)}$) to cause
 15 a switch to infinite optimal rotation length to occur (compare Figure 3 (c) and Figure 5).

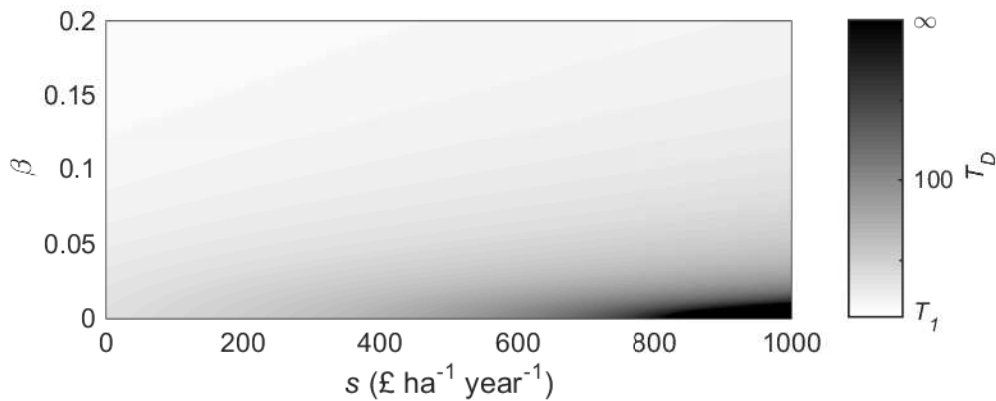


Figure 5: How the optimal rotation length is affected by the green payment being dependent on the level of infection in the forest. The optimal rotation length, T_D , is shown as the gradation in black-white shading across the in a $s - \beta$ parameter space (corresponding to variation in the relative value of disease transmission and green payments for non-timber benefits). The grey-scale on the right-hand side indicates the optimal rotation length (T_D) with the lower boundary equal to the minimum harvesting boundary, T_1 (white) and the upper boundary equalling an infinite rotation length (black). The green payment is dependent on the level of infection in the forest giving $S(L) = s\tilde{L}(T)$ in Equation (5). The external pressure is set at the baseline value (see Table 2), and all other parameters are given in Table 1.

1 6 Summary and discussion

2 The interaction between the effects of the green payment and disease characteristics is the central issue for this
3 paper. We analysed the NPV of a forest where a disease arrived during the rotation, and found that the optimal
4 rotation length is obtained when the marginal benefit of waiting for one more instant of timber growth and of
5 green payment, is equal to the opportunities forgone and the marginal cost of disease spreading further (section
6 2). In Macpherson et al. (2016) we showed that when timber from infected trees has no value, disease generally
7 decreases the optimal rotation length. However, here we show that the inclusion of a green payment based on
8 the area of the current tree crop that is retained unharvested, counteracts the effect of disease, since the green
9 payment incentivises the owner to delay harvesting. Moreover, at some critical level of green payment, the
10 optimal rotation length becomes infinite. The faster the disease spreads, the smaller the critical green payment
11 needed to generate an infinite optimal rotation length (Figure 3). Interestingly, the effect of forest carbon
12 payments, which has been explored many times before, has also been found to increase the optimal rotation
13 length (in the absence of disease) and in some cases make it optimal never to harvest (Van Kooten et al., 1995;
14 Price and Willis, 2011).

15 When the timber from infected trees has a positive value, we found an interesting interaction between the
16 impacts of disease spread, the effect of disease on timber value and the non-timber benefits on optimal rotation
17 length. Decreasing the value of timber from infected trees can result in either an increase or a decrease in the
18 optimal rotation length dependent on the level of green payment (Figure 4). In summary, we have shown that
19 the inclusion of an annual, green payment for the non-timber benefits of the forest will increase the optimal
20 rotation length. This acts in the opposite direction to disease and creates a trade-off between (i) waiting for
21 the disease to spread further and accruing more non-timber benefits and (ii) harvesting earlier to maximise the
22 revenue from timber of infected trees.

23 In section 5 we tested the effect of the green payment being dependent on the infection status of the forest
24 and show that, in this case, the disease will most likely decrease the optimal rotation length and the switch
25 to the optimal rotation length being infinite only occurs at much higher levels of green payment. This is a
26 key result and highlights the importance of model formulation, and that when modelling specific host-pathogen
27 systems, the effect of disease on both timber and non-timber benefits should be considered carefully.

28 Several papers have examined the effect of catastrophic, abiotic events on forest owners' decision-making
29 (Reed, 1984; Englin et al., 2000; Amacher et al., 2005, 2009). Englin et al. (2000) carried out an empirical
30 study using a Faustmann framework to find the effect of fire risk on a Jack pine in the Canadian Shield region.
31 He included the cost of non-timber benefits (obtained through wilderness recreation), and found that while
32 the presence of fire risk shortens the optimal rotation length, the inclusion of the non-timber benefits had an
33 opposite effect and increased the optimal rotation length. Whilst we have a different model formulation (our

1 framework is deterministic opposed to stochastic), our overall results have notably similarities with those of
2 Englin et al. (2000), but our finding of parameter spaces where the optimal rotation length becomes infinite
3 were not found by Englin et al. (2000).

4 Our findings are important because it demonstrates the complex interaction between the timber and non-
5 timber values of a forest in the presence of tree disease. However we have excluded many complexities, such as
6 multiple rotations, in order to examine this interaction clearly. We now address these simplifications and future
7 work. Most optimal rotation length work considers multiple rotations where trees are perpetually planted and
8 harvested thus synonymously including the benefit of the land ('land rent'). The inclusion of multiple rotation
9 analysis in the traditional sense (calculating the NPV over infinite forest rotations), requires detailed knowledge
10 of the persistence of disease between rotations. For example, can the infected material live in the environment
11 after harvesting so that it affects future rotations; and if so how does this pressure change between rotations?
12 Moreover, if the disease does not carry over to the future rotations, then arguably the optimal rotation length of
13 the rotation with disease would be different from all future rotations without disease. Thus, the simplest way to
14 extend this model to include land rent from future rotations is to assume an annual payment after the harvest
15 at the end of the rotation. This can represent changing the land use or changing the tree species planted in the
16 following rotation, which may be necessary after an epidemic which retains infectious material within the site
17 (such as *Heterobasidion annosum*; Pratt (2001); Redfern et al. (2010)).

18 It is interesting to note that, without the green payment, the optimum solution to the arrival of tree disease
19 is to shorten the rotation length, which not only reduces loss from timber revenue, but also removes a source
20 of infection, which may in turn reduce the transmission of the disease to neighbouring forests. In contrast the
21 inclusion of a green payment increases the optimal rotation length and thus the period of time that infected
22 trees are left standing and thus potentially acting as a reservoir of infection that can spread to surrounding
23 forests. It also increases the exposure time of these unhealthy (or even dead) trees to further disturbances such
24 as fire, wind, pests and other pathogens (Spittlehouse and Stewart, 2004). Never harvesting an infected forest
25 would be seen by many as irresponsible, especially for fast-spreading epidemics, and is contrary to government
26 prescriptions for some diseases such as *P. ramorum* in Great Britain (Forestry Commission Scotland, 2015).

27 This highlights the importance of scaling and we are cautious of interpreting a strategy which was optimised
28 from a single forest owner's perspective at a landscape scale. To do this would require a different model
29 framework since the decision to harvest in each forest affects the risk of disease transmission to neighbouring
30 forests. One such framework is to use a network model (Keeling and Eames, 2005). The nodes on the network
31 represent forest patches, owned by different managers, and are connected dependent on how the disease spreads.
32 For example, if infected inoculum disperse locally via spores then the distance between patches can be used to
33 determine the strength of connection and the likelihood of an un-infected patch becoming infected. Each forest
34 manager decides when to harvest their patch by maximising their forest patches NPV (private strategy). Thus

1 the decision of when to harvest a patch will be dependent not only on the patches infection status, but also on
2 the connected neighbours' patches infection status and harvesting decisions. This model could be contrasted
3 with a social planner's optimal strategy, where the social planner maximises the NPV of the network of patches.
4 More specifically, if a government body or large organisation managed the network of patches, how would
5 the optimal rotation length of each patch be different compared to the private strategy? This concept has
6 been examined before when considering how best to deploy surveillance methods, or controls to halt biological
7 invasions (Bhat et al., 1996; Burnett et al., 2006; Epanchin-Niell et al., 2009; Epanchin-Niell and Wilen, 2014),
8 but we are not aware of any papers examining the optimal rotation length in on a landscape of forests under
9 different management areas (such as the private or social planner).

10 **Acknowledgements**

11 This work is from the project titled Modelling economic impact and strategies to increase resilience against tree
12 disease outbreaks. Funded jointly by a grant from BBSRC, Defra, ESRC, the Forestry Commission, NERC and
13 the Scottish Government, under the Tree Health and Plant Biosecurity Initiative.

1 References

- 2 Alvarez, L. and Koskela, E. (2006). Does risk aversion accelerate optimal forest rotation under uncertainty?
3 *Journal of Forest Economics*, 12(3):171–184.
- 4 Amacher, G., Ollikainen, M., and Koskela, E. (2009). *Economics of forest resources*. Mit Press Cambridge.
- 5 Amacher, G. S., Malik, A. S., and Haight, R. G. (2005). Not getting burned: the importance of fire prevention
6 in forest management. *Land Economics*, 81(2):284–302.
- 7 Appiah, A., Jennings, P., and Turner, J. (2004). Phytophthora ramorum: one pathogen and many diseases, an
8 emerging threat to forest ecosystems and ornamental plant life. *Mycologist*, 18(4):145–150.
- 9 Bauce, É. and Fuentealba, A. (2013). Interactions between stand thinning, site quality and host tree species on
10 spruce budworm biological performance and host tree resistance over a 6 year period after thinning. *Forest
11 Ecology and Management*, 304:212–223.
- 12 Bhat, M. G., Huffaker, R. G., and Lenhart, S. M. (1996). Controlling transboundary wildlife damage: modeling
13 under alternative management scenarios. *Ecological modelling*, 92(2):215–224.
- 14 Boyd, I., Freer-Smith, P., Gilligan, C., and Godfray, H. (2013). The consequence of tree pests and diseases for
15 ecosystem services. *Science*, 342(6160):1235773.
- 16 Burnett, K. M. et al. (2006). Introductions of invasive species: failure of the weaker link. *Agricultural and
17 Resource Economics Review*, 35(1):21.
- 18 Carvalho-Santos, C., Honrado, J., and Hein, L. (2014). Hydrological services and the role of forests: Con-
19 ceptualization and indicator-based analysis with an illustration at a regional scale. *Ecological Complexity*,
20 20:69–80.
- 21 Castagneyrol, B., Jactel, H., Vacher, C., Brockerhoff, E., and Koricheva, J. (2014). Effects of plant phylogenetic
22 diversity on herbivory depend on herbivore specialization. *Journal of applied ecology*, 51(1):134–141.
- 23 Chladná, Z. (2007). Determination of optimal rotation period under stochastic wood and carbon prices. *Forest
24 Policy and Economics*, 9(8):1031–1045.
- 25 Churchill, D. J., Larson, A., Dahlgreen, M., Franklin, J., Hessburg, P., and Lutz, J. (2013). Restoring forest
26 resilience: From reference spatial patterns to silvicultural prescriptions and monitoring. *Forest Ecology and
27 Management*, 291:442–457.
- 28 Condeso, T. and Meentemeyer, R. (2007). Effects of landscape heterogeneity on the emerging forest disease
29 sudden oak death. *Journal of Ecology*, 95(2):364–375.

- 1 Cudlín, P., Seják, J., Pokorný, J., Albrechtová, J., Bastian, O., and Marek, M. (2013). Forest ecosystem services
2 under climate change and air pollution. In *Climate Change, Air Pollution and Global Challenges*, chapter 24,
3 pages 521–546. Elsevier.
- 4 D’Amato, A. W., Troumbly, S., Saunders, M. R., Puettmann, K., and Albers, M. (2011). Growth and survival
5 of picea glauca following thinning of plantations affected by eastern spruce budworm. *Northern Journal of*
6 *Applied Forestry*, 28(2):72–78.
- 7 Department for Environment, Food and Rural Affairs (2013). Tree Health and Plant Biosecurity Expert Task-
8 force: Final report. (March).
- 9 Englin, J., Boxall, P., and Hauer, G. (2000). An empirical examination of optimal rotations in a multiple-use
10 forest in the presence of fire risk. *Journal of agricultural and resource economics*, pages 14–27.
- 11 Epanchin-Niell, R. S., Hufford, M. B., Aslan, C. E., Sexton, J. P., Port, J. D., and Waring, T. M. (2009).
12 Controlling invasive species in complex social landscapes. *Frontiers in Ecology and the Environment*, 8(4):210–
13 216.
- 14 Epanchin-Niell, R. S. and Wilen, J. E. (2014). Individual and cooperative management of invasive species in
15 human-mediated landscapes. *American Journal of Agricultural Economics*, page aau058.
- 16 Forest Research, *Private communication* (2015).
- 17 Forestry Commission (2011). NFI 2011 woodland map Scotland.
- 18 Forestry Commission Scotland (2013). Dothistroma Needle Blight Action Plan for Scotland.
- 19 Forestry Commission Scotland (2015). Action Plan for Ramorum on Larch Scotland.
- 20 Hartman, R. (1976). The harvesting decision when a standing forest has value. *Economic inquiry*, 14(1):52–58.
- 21 Jactel, H. and Brockerhoff, E. G. (2007). Tree diversity reduces herbivory by forest insects. *Ecology letters*,
22 10(9):835–848.
- 23 Johansson, S., Pratt, J., and Asiegbu, F. (2002). Treatment of norway spruce and scots pine stumps with urea
24 against the root and butt rot fungus heterobasidion annosum – possible modes of action. *Forest ecology and*
25 *management*, 157(1):87–100.
- 26 Johansson, T., Hjältén, J., de Jong, J., and von Stedingk, H. (2013). Environmental considerations from
27 legislation and certification in managed forest stands: A review of their importance for biodiversity. *Forest*
28 *Ecology and Management*, 303:98–112.

- 1 Keeling, M. J. and Eames, K. T. (2005). Networks and epidemic models. *Journal of the Royal Society Interface*,
2 2(4):295–307.
- 3 Koskela, E. and Ollikainen, M. (2001). Optimal private and public harvesting under spatial and temporal
4 interdependence. *Forest Science*, 47(4):484–496.
- 5 Loisel, P. (2011). Faustmann rotation and population dynamics in the presence of a risk of destructive events.
6 *Journal of forest economics*, 17(3):235–247.
- 7 Macpherson, M., Kleczkowski, A., Healey, J., and Hanley, N. (2016). When to harvest? the effect of disease on
8 optimal forest rotation. *University of St. Andrews, Environmental Economics Discussion Papers*.
- 9 Millar, C. I., Stephenson, N. L., and Stephens, S. L. (2007). Climate change and forests of the future: managing
10 in the face of uncertainty. *Ecological applications*, 17(8):2145–2151.
- 11 Netherer, S. and Schopf, A. (2010). Potential effects of climate change on insect herbivores in european forests
12 – general aspects and the pine processionary moth as specific example. *Forest Ecology and Management*,
13 259(4):831–838.
- 14 Newman, D. (2002). Forestry’s golden rule and the development of the optimal forest rotation literature. *Journal*
15 *of Forest Economics*, 8(1):5–27.
- 16 Nielsen, A. B., Olsen, S. B., and Lundhede, T. (2007). An economic valuation of the recreational benefits
17 associated with nature-based forest management practices. *Landscape and urban planning*, 80(1):63–71.
- 18 Pautasso, M., Aas, G., Queloz, V., and Holdenrieder, O. (2013). European ash (*fraxinus excelsior*) dieback—a
19 conservation biology challenge. *Biological Conservation*, 158:37–49.
- 20 Pautasso, M., Dehnen-Schmutz, K., Holdenrieder, O., Pietravalle, S., Salama, N., Jeger, M., Lange, E., and
21 Hehl-Lange, S. (2010). Plant health and global change – some implications for landscape management.
22 *Biological Reviews*, 85(4):729–755.
- 23 Perry, D. A. and Maghembe, J. (1989). Ecosystem concepts and current trends in forest management: time for
24 reappraisal. *Forest Ecology and Management*, 26(2):123–140.
- 25 Pratt, J. (2001). Stump treatment against fomes. *Forest Research: Annual Report and Accounts*, 2002:76–85.
- 26 Price, C. (2011). When and to what extent do risk premia work? cases of threat and optimal rotation. *Journal*
27 *of forest economics*, 17(1):53–66.
- 28 Price, C. and Willis, R. (2011). The multiple effects of carbon values on optimal rotation. *Journal of forest*
29 *economics*, 17(3):298–306.

- 1 Quine, C., Marzano, M., Fuller, L., Dandy, N., Porth, E., Jones, G., Price, C., Barnett, J., and Brandon, G.
2 (2015). Social and economic analyses of Dothistroma Needle Blight.
- 3 Redfern, D., Pratt, J., Hendry, S., and Low, J. (2010). Development of a policy and strategy for controlling
4 infection by *Heterobasidion annosum* in British forests: a review of supporting research. *Forestry*, cpq005.
- 5 Reed, W. (1984). The effects of the risk of fire on the optimal rotation of a forest. *Journal of Environmental*
6 *Economics and Management*, 11(2):180–190.
- 7 Ribe, R. G. (1989). The aesthetics of forestry: what has empirical preference research taught us? *Environmental*
8 *management*, 13(1):55–74.
- 9 Rizzo, D. M. and Garbelotto, M. (2003). Sudden oak death: endangering california and oregon forest ecosystems.
10 *Frontiers in Ecology and the Environment*, 1(4):197–204.
- 11 Samuelson, P. (1976). Economics of forestry in an evolving society. *Economic Inquiry*, 14(4):466–492.
- 12 Sims, C. and Finnoff, D. (2013). When is a “wait and see” approach to invasive species justified? *Resource and*
13 *Energy Economics*, 35(3):235–255.
- 14 Spittlehouse, D. L. and Stewart, R. B. (2004). Adaptation to climate change in forest management. *Journal of*
15 *Ecosystems and Management*, 4(1).
- 16 Sturrock, R. (2012). Climate change and forest diseases: using today’s knowledge to address future challenges.
17 *Forest Systems*, 21(2):329–336.
- 18 Sturrock, R., Frankel, S., Brown, A., Hennon, P., Kliejunas, J., Lewis, K., Worrall, J., and Woods, A. (2011).
19 Climate change and forest diseases. *Plant Pathology*, 60(1):133–149.
- 20 Van Kooten, G. C., Binkley, C. S., and Delcourt, G. (1995). Effect of carbon taxes and subsidies on optimal
21 forest rotation age and supply of carbon services. *American Journal of Agricultural Economics*, 77(2):365–374.